



## Design of a Real-Time Monitoring and Controlling System for the PEM Fuel Cell Model Based on LabVIEW with IoT Technology

Fatima Abdul Sattar AL-Taie<sup>1\*</sup>      Ahmed Sabah Al-Araji<sup>1</sup>

<sup>1</sup> Computer Engineering Department, University of Technology –Iraq, Baghdad, Iraq

\* Corresponding author's Email: 120121@uotechnology.edu.iq

---

**Abstract:** In this research, a predictive voltage neural controller and remote monitoring for the nonlinear proton exchange membrane fuel cell (PEMFC) system are implemented in real-time. This paper's major purpose is to precisely and rapidly determine the appropriate hydrogen partial pressure (PH<sub>2</sub>) control action to improve the fuel cell's nonlinear performance under varying load currents and to enable remote monitoring of the nonlinear PEMFC system based on the internet of things (IoT). The laboratory, virtual instrument engineering workbench (LabVIEW) package is used to demonstrate the real-time performance of the proposed predictive voltage controller applied to the 150-watt PROTIUM PEMFC, which will be used to generate the appropriate amount of hydrogen partial pressure control action that will enter the fuel cell for stabilizing the desired output voltage. The message queuing telemetry transport (MQTT) protocol and a Raspberry Pi 4 acting as a local server are the building blocks upon which the monitoring component of the proposed system is implemented in order to monitor the desired output voltage, the fuel cell output voltage, and PH<sub>2</sub>. The Raspberry Pi collects the necessary fuel cell data and sends it to the node-red dashboard for monitoring. According to the simulation and the experimental results obtained using the proposed predictive controller on PROTIUM PEMFC, the proposed controller can generate an accurate, prompt, and timely reaction to the hydrogen partial pressure control action to reduce the tracking voltage error and to get rid of the fuel cell output voltage oscillation. The proposed experimental work was compared to the simulation findings to confirm its effectiveness in terms of effectively tracking the desired output voltage, providing a fast response, and achieving the optimal partial pressure of hydrogen. However, in the simulation findings, a voltage error of 0.01 volts was observed without any oscillation. On the other hand, the experimental results indicate a slightly higher voltage error of approximately 0.1 volts, accompanied by oscillations of around  $\pm 0.1$  volts.

**Keywords:** Predictive controller, PEMFC model, Monitoring and controlling, IOT, MQTT, LabVIEW, Node-RED.

---

### 1. Introduction

Due to the negative environmental effects of fossil fuels, the world is now investigating new energy generation methods. In particular, renewable energy is still the main focus and is seen as the best alternative to fossil fuels [1]. In this context, hydrogen fuel cells are attracting global interest that is only going to grow because of their high energy density, low construction costs, and low air pollution [2]. Specifically, the use of the fuel cell (FC) technology is considered a sustainable energy option, known for its eco-friendly characteristics and long lifespan. It is recognized as a green energy solution

due to its minimal environmental impact and emission-free nature [3]. The fuel cell's basic operating principle is the production of straightforward electrical energy as a result of a chemical process. In particular, the PEMFC systems are the most popular hydrogen energy source because they offer the essential qualities of high efficiency, high reliability, low operating noise, and flexible modular design together with excellent performance, quick power response, high power density, low operating temperature, and low maintenance requirements. Consequently, they are widely utilized in military environments, cars, unmanned aerial vehicles, and mobile devices [4, 2]. Therefore, achieving optimum fuel cell efficiency in the

presence of multiple factors that impact the cell's performance is the main difficulty for many researchers. For instance, the fuel cell is affected by factors including fuel pressure, temperature, humidity, and applied current, which results in nonlinear dynamic behaviour in the system's generation [5]. Moreover, since the fuel cell's output voltage varies with the step change, the load current is regarded as a critical problem in the nonlinear fuel cell behaviour. For this reason, a controller that generates the proper value of  $P_{H_2}$  is required in order to supply the necessary voltage during variations in the load current [2].

Moreover, monitoring and control of a PEMFC are essential to optimizing efficiency, safety, durability, and cost. They can help prevent safety hazards, identify and address issues that can reduce lifespan, and reduce operating costs [5, 6]. Typically, real-time monitoring gives users instant access to a variety of data sources, and this lowers the danger of acting too late when an unforeseen incident occurs by enabling users to make judgments and take action more quickly [7]. Thus, to ensure PEMFC safety and to improve system efficiency, performance monitoring is a crucial requirement. In this regard, scholars have suggested a variety of fuel cell control and monitoring methods. For example, to increase the efficiency of PEMFC, the authors in [8] presented a comprehensive study of the effect of temperature on proton exchange membrane (PEM) water electrolysis and PEM fuel cells. The study was carried out using a wireless LoRa node and the gateway network concept to monitor and control the temperature level of the fuel cell system. It is worth noting that the study's focus is on monitoring and operating the fuel cell system rather than its design or optimization. Generally, using LoRa for real-time monitoring of PEMFC has the disadvantage of a low data transmission rate compared to Wi-Fi, which limits the frequency and speed of data updates. Additionally, the long-range nature of LoRa can introduce latency in transmitting temperature data, making it unsuitable for real-time monitoring and applications requiring high-resolution data.

To ensure high safety and reliability standards, the authors in [9] proposed a method for calculating the proton exchange membrane fuel cells' remaining usable life (RUL) based on monitoring data. Based on monitoring data, the research presented a stochastic degradation model for PEMFCs, and they applied it to forecast the RUL of the fuel cell. In particular, the research uses highly accurate simulation results to show that the suggested strategy is feasible. A hybrid PEM fuel cell system with Li-ion batteries and an LPG (liquefied petroleum gas)

reformer was suggested in [10] utilizing a supervisory control and monitoring system. The system was developed to assure both safe operation and fuel cell system performance optimization. To improve the effectiveness of fuel cells, the researchers in [11] described the application of differential evolution-based impedance spectroscopy for accurate fault monitoring and detection in PEMFC single cells and stacks. The suggested system uses DEIS (dynamic electrochemical impedance spectroscopy) to track the PEMFCs' impedance and find any possible faults. A fractional-order PID (FOPID) controller was suggested in [12] to enhance the dynamic performance and effectiveness of the proton exchange membrane fuel cell. Specifically, the PEMFC output voltage was controlled using hydrogen pressure as a control variable. Additionally, a real-time virtual test system based on the LabVIEW simulation interface toolkit and MATLAB/Simulink was used to assess the PEMFC control system's functionality.

Furthermore, in [13], a researcher proposed the utilization of a voltage-tracking controller to enhance the dynamic response of the output voltage in PEMFC systems. This was achieved through the application of an inverse neural controller and an HFF-CPSO (hybrid firefly chaotic particulate swarm optimization) algorithm, which aimed to provide a smoother control action for  $P_{H_2}$  and reduce output voltage oscillation. However, due to the reliance on a conventional identifier and the limited effectiveness of the inverse neural controller, acceptable responses were only generated in steady-state conditions, while errors persisted in transient states. As a result, complete elimination of output voltage oscillation was not achieved, and a small error value remained in the output voltage. In addition, the authors in [14] outlined a methodology for improving the PEM fuel cell performance by employing controlled short-circuiting. Particularly, they designed and fabricated an Arduino shield-like module to read individual voltages and intervene when a cell's performance shifts outside the expected range. However, it is important to note that the proposed method is still in the prototype stage and requires further testing and integration with an electric energy generator to improve the supervision and actuation algorithms. Further, there is no real-time remote monitoring for the PEMFC. A mathematical model for real-time monitoring of automotive PEM fuel cells was presented in [6] in order to increase the fuel cell's efficiency and lengthen its useful lifespan. This model achieves computational efficiency through the spatio-temporal decoupling of the problem, creating a new variable for cathode catalyst use and a new

reduced-order model for water balance across the membrane electrode assembly (MEA). The authors in [15] described the creation of a fault detection method and an online condition monitoring system for PEMFCs based on electrochemical impedance spectroscopy readings. The research suggested a condition monitoring method for PEMFCs that uses the stack impedance at a certain frequency for problem detection and reports the systems' overall health using an EIS (electrochemical impedance spectroscopy)-based fault diagnostic method employing fuzzy logic. The proposed approach is found to have the ability to diagnose faults in PEMFCs, but there is a degree of inaccurate monitoring and diagnostic accuracy, as well as a lack of remote monitoring for the PEMFC. The research presented in [16] proposes the utilization of a neural predictive controller with CPSO to determine the appropriate  $P_{H_2}$  action in response to changes in the load current, aiming to achieve the desired output voltage of the PEMFC system. While the actual output voltage of the PEMFC system could track the desired output with a one-step-ahead prediction, certain issues were observed. These included a small output oscillation, a non-zero voltage error in steady-state, an overshoot response in the initial sample, and an unsteady response from the control action  $P_{H_2}$ . In order to address these limitations and enhance system performance, the authors extended the prediction horizon to 10 steps to obtain the optimal response. However, this approach resulted in increased processing time and slower overall action. In [17], an active fault-tolerant control method-based health management strategy for PEM fuel cells was explained. For condition monitoring and error diagnosis, the method employs a stack voltage model and quick electrochemical impedance spectroscopy. Then, they stated that there are three common fuel cell problems that can be identified and corrected using the suggested method. In order to detect the performance heterogeneity of a PEMFC during operation and to monitor PEMFC performance heterogeneity to ensure its safety and enhance system efficiency, the researchers in [18] used magnetic field imaging as an online and non-destructive method upon the establishment of the association between PEMFC performance and magnetic field variation. In addition, computational models and experimental validation in various PEMFC failure scenarios were conducted and the fluctuation in the output voltage of the fuel cell increases with small values. The IoT has received close attention from researchers, and it is anticipated that the IoT will link billions of consumers with trillions of pieces of networked equipment that will interact in real-time [19]. In

particular, IoT has emerged as a key technology that enables communication between humans and all kinds of items, machines, and other things. The Internet of Things is a system made up of physical objects and sensors attached to or coupled with those objects that are connected to the Internet via wired and wireless network architectures. The connected devices require a protocol so that they can only communicate when necessary [20].

In this work, the problem definition is that the output voltage of the fuel cell varies with varying load current and is regarded as a critical problem in nonlinear fuel cell behaviour. As a consequence, a controller that generates the proper value of  $P_{H_2}$  is required in order to supply the necessary voltage during variations in the load current.

This study's specific objective is to identify the best control action value for the  $P_{H_2}$  in order to prolong the life of the fuel cell, improve the dynamic performance of the nonlinear fuel cell output voltage, and significantly reduce hydrogen consumption. This can be accomplished by putting into practice the suggested predictive neural controller that was presented in [2]. In addition, real-time remote monitoring of the PEMFC's performance via the IoT technique is implemented in this work.

The primary contribution of this study is to:

- Investigate and assess how changes in the input value of the  $P_{H_2}$ , the fuel cell's output current, and temperature affect the nonlinear PEMFC model's output voltage to study and analyse the characteristic of the PEM fuel cell model of type PROTIUM.
- Experimentally implement the one-step-ahead predictive controller that was suggested in [2] based on the LabVIEW simulation interface toolkit (front panel and block diagram), to generate a suitable value of  $P_{H_2}$  and to track and stabilize the desired output voltage of the fuel cell.
- Develop a real-time monitoring system based on the IoT utilizing the MQTT communication protocol and a node-red monitoring dashboard to send the value of  $P_{H_2}$ , the desired voltage, and the fuel cell output voltage, and monitor them.

The rest of the article is organized as follows: The PROTIUM PEMFC nonlinear model is provided in section 2. The proposed monitoring and control system design is explained in section 3. Section 4 describes the experimental setup that has been implemented, and section 5 describes the simulation and experimental outcomes of this work. Finally, section 6 discusses the work's conclusions.

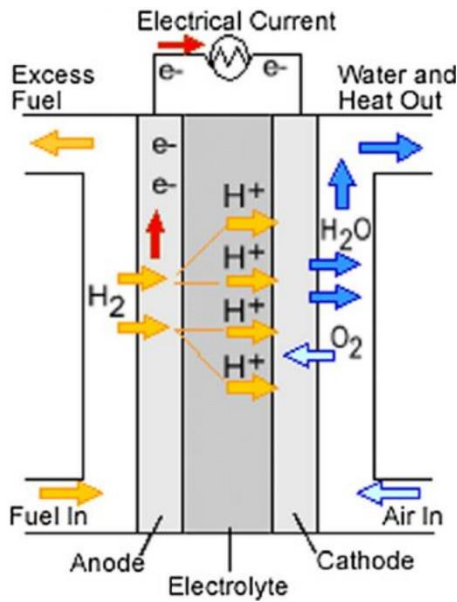


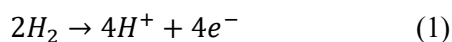
Figure. 1 The structure of the PEMFC chemical process [5]

Table 1. The physical parameters of the fuel cell [2]

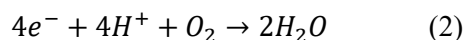
Parameters	Values	Units
$N_{cell}$	25	--
$T$	298	K
$A$	21.3	$cm^2$
$L$	$178 \times 10^{-6}$	$cm$
$PH_2$	0-1	Bar
$PO_2$	0.2	Bar
$R_c$	0.0003	$\Omega$
$B$	0.0169	Volt
$\alpha_1$	0.948	Volt
$\alpha_2$	0.00312	Volt/k
$\alpha_3$	$7.6 \times 10^{-5}$	Volt.K <sup>-1</sup> . Mol <sup>-1</sup> /cm <sup>3</sup>
$\alpha_4$	$-1.93 \times 10^{-4}$	Volt.K <sup>-1</sup> /A
$J$	0.0073	$mA/cm^2$
$J_{max}$	0.469	$mA/cm^2$
$\Phi$	23	--

## 2. PEM fuel cell nonlinear model

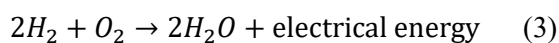
PEMFCs use chemical processes to produce electrical energy without releasing any unwanted by-products. Fig. 1 depicts the PEMFC model's structure as seen from the perspective of the chemical reaction [5]. This specific kind of cell depends on a distinctive, unique polymer membrane covered in widely distributed catalyst particles. Hydrogen is injected into the membrane from the anode side, where the catalyst causes the hydrogen atoms to lose their electrons and change into protons ( $H^+$ ) ions. According to Eq. (1), the chemical process taking place at the anode is as follows [21]:



The proton exchange membrane allows only  $H^+$  ions to pass through, and before they reach the cathode side, the electrons go to an external circuit to provide the output voltage. To make water, hydrogen ions and oxygen from the air are combined with electrons. Eq. (2) shows the chemical reaction taking place at the cathode [2]:



In Eq. (3), the overall reaction is expressed as follows [2, 21]:



Under normal operating conditions, a single cell generates between 0.5 and 0.9 volts. Since more power is required, multiple cells are connected

serially as necessary to form a "stack," and a stack arrangement can have a power output of hundreds of kilowatts. The output voltage of a single cell is described as follows [2, 5]:

$$V_{cell} = V_{steady} - V_{transient} \quad (4)$$

$$V_{steady} = E_N - V_{ohm} \quad (5)$$

$$V_{transient} = V_{act} + V_{con} \quad (6)$$

Where  $V_{cell}$  is a fuel cell's output voltage,  $V_{ohm}$  is the ohmic voltage drop brought on by the resistance to protons and electrons passing through the solid electrolyte,  $V_{act}$  is the voltage drop brought on by anode and cathode activation, and  $V_{con}$  is the voltage drop brought on by a decrease in the concentration of the reactants' gases or the passage of mass of oxygen and hydrogen.  $E_N$  is also known as the cell's thermodynamic potential or the reversible voltage and may be calculated as follows [21]:

$$E_N = 1.229 + 4.3085 \times 10^{-5} \times T \times (\ln PH_2 + 0.5 \ln PO_2) - 0.85 \times 10^{-3} \times (T - 298) \quad (7)$$

Where  $PH_2$  and  $PO_2$  are the respective partial pressures of hydrogen and oxygen, and  $T$  is the fuel cell temperature expressed in Kelvin (K) [2, 5]. The physical fuel cell characteristics shown in Table 1 can be used to determine each term in Eq.s (4-6). The stack's total output voltage can be calculated using Eq. (8) [2]:

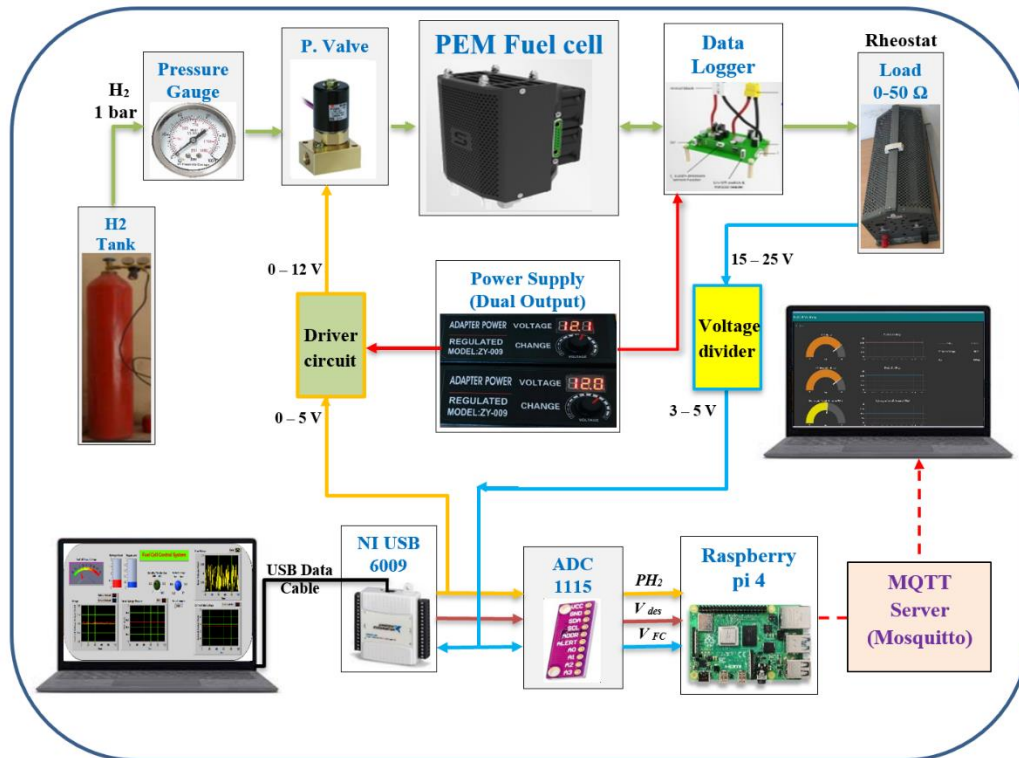


Figure 2. The schematic diagram of the proposed PEMFC monitoring and control system for the proposed experimental work

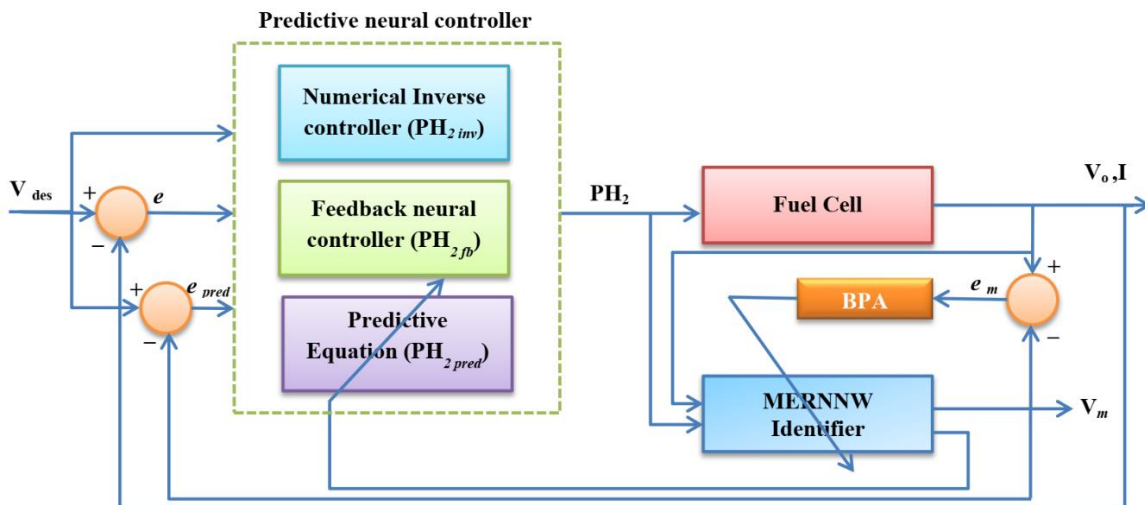


Figure. 3 The proposed predictive voltage control strategy structure [2]

$$V_{FC} = N_{cell} \times V_{cell} \quad (8)$$

Where  $N_{cell}$  is the number of cells in the stack.

### 3. Monitoring and control system design

Fig. 2 depicts the schematic diagram of the proposed PEMFC monitoring and control system used in the experimental work. It consists of multiple proposed components (hardware and software). Therefore, the LabVIEW program is used to create the control section for the proposed monitoring and

control system, which is utilized to verify the performance of the proposed predictive neural controller in controlling the fuel cell output voltage in real time by generating the appropriate amount of hydrogen partial pressure control action that will enter the fuel cell.

The monitoring portion of the suggested system is implemented based on the MQTT protocol and a Raspberry Pi 4 as a local server. In the short term, the Raspberry Pi gathers the required fuel cell data and transmits it to the dashboard for monitoring. The

monitoring dashboard uses Node-Red and the MQTT protocol for data exchange and communication between the MQTT clients, and it is used to receive and visualize the obtained FC data over the web and the Wi-Fi connection.

The design of the controller and the monitoring system, as well as the methods utilized to implement them, will be described in depth in the following subsections.

### 3.1 The predictive voltage controller

Our proposed predictive voltage controller for the general form of the PEMFC is depicted in Fig. 3, which has been taken from our work in [2]. We have provided a detailed explanation of the proposed predictive neural controller design in reference [2]. Basically, this controller's main task is to solve the problem of the fuel cell's output voltage variation while the load current varies by generating the best value of  $PH_2$ , which is fed to the fuel cell to obtain the necessary voltage during variations in the load current. The suggested predictive voltage controller comprises three sub-controllers. The first sub-controller, known as the numerical feed-forward controller (NFFC), determines the hydrogen partial pressure control action required for steady-state based on the desired voltage. The second sub-controller, which is a feedback neural controller, uses a multi-layer perceptron (MLP) and a back-propagation learning algorithm to generate the  $PH_2$  feedback control action during transient conditions to follow the desired FC output voltage. The third sub-controller is the predictive control law equation, which utilizes the modified Elman recurrent neural network (MERNN) as an identifier for the PEMFC model and the multi-objective performance index. Essentially, the proposed predictive control law equation of the nonlinear fuel cell model is provided the third sub-controller is the predictive control law equation, which utilizes the modified Elman recurrent neural network (MERNN) as an identifier for the PEMFC model and the multi-objective performance index. Essentially, the proposed predictive control law equation of the nonlinear fuel cell model is provided for the one-step ahead prediction, as represented in Eq. (9) in order to obtain the optimal or near-optimal value for the hydrogen partial pressure control effort.

$$PH_{2pred}(k+1) = PH_{2pred}(k) + \eta Q e_{pred}(k+1) \times \left[ \sum_{j=1}^{nh} w_{6j} f'(net_j) VH_{j6} \right] - \eta R [PH_{2fb}(k) + PH_{2pred}(k)] \quad (9)$$

Where  $PH_{2pred}(k+1)$  is the hydrogen partial pressure control action for one step ahead prediction,  $\eta$  is the learning rate,  $PH_{2fb}$  is the feedback hydrogen partial pressure control action,  $e_{pred}$  represents the voltage error, Q and R represent the positive weight coefficients for the predictive control law equation [22],  $nh$  denotes the number of nodes in the hidden layer,  $w_{6j}$  is the weight of the input layer related to the  $PH_2$  input node,  $VH_{j6}$  describes the weight of the hidden layer node,  $net_j$  is the weighted sum in the hidden layer, and  $f'$  is the first derivative function. As a results, this control effort will track and stabilize the fuel cell's output voltage model at the desired output voltage in the two states: The transient and the steady-state operations.

The predictive voltage controller program was created using the LabVIEW 2020 package, and it was specifically created to meet the needs of the experimental goal of managing the hydrogen partial pressure that enters the fuel cell. LabVIEW is the National Instruments' visual programming language for a system design platform and development environment.

LabVIEW is frequently used for data gathering, instrument control, and industrial automation on a variety of operating systems (OSs), including Microsoft Windows, several versions of Unix, Linux, and MacOS. LabVIEW initially became available for the Apple Macintosh in 1986 [23]. Furthermore, it is recognized as the most popular software environment monitoring tool. The LabVIEW interface software diagram includes the primary program in the form of a Graphic User Interface (GUI), which runs all of the controls and indicators on the front panel [24]. In general terms, the performance of the proposed controller was tested and evaluated in real time based on the LabVIEW toolkit. The benefit of a real-time test system is that it allows us to examine the functioning state under various disturbances and monitor the performance of the PEMFC control system from a single panel [12].

Figs. 4 and 5 show the front panel and the block diagram, respectively, of the proposed predictive voltage controller, which has been constructed as described in those images based on the LabVIEW tool kit.

### 3.2 Monitoring system design

This section explains the remote monitoring system architecture that has been implemented in the experimental work, which is shown in Fig. 6. The MQTT communication protocol has been utilized to transmit the required fuel cell monitoring data. Fig. 7

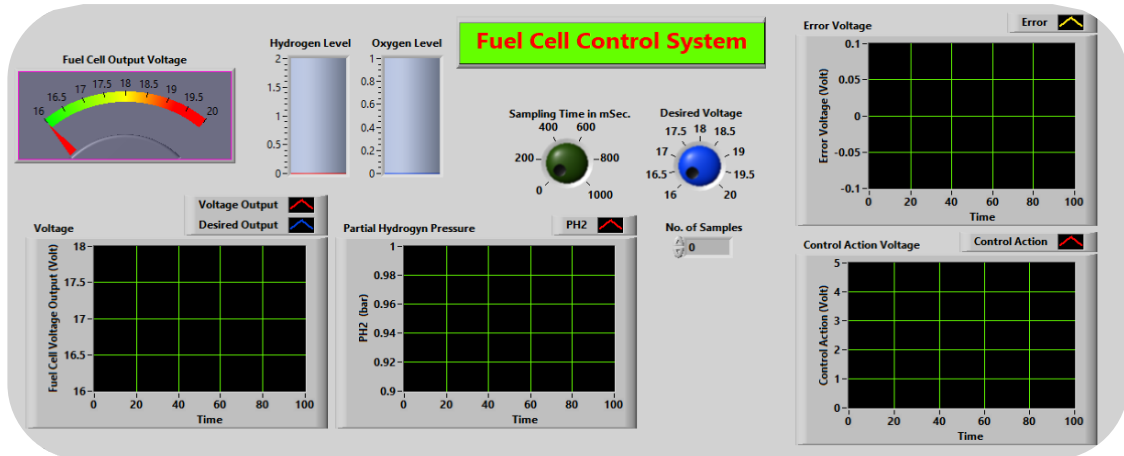


Figure. 4 Front panel for the real-time PEMFC predictive controller in LabVIEW

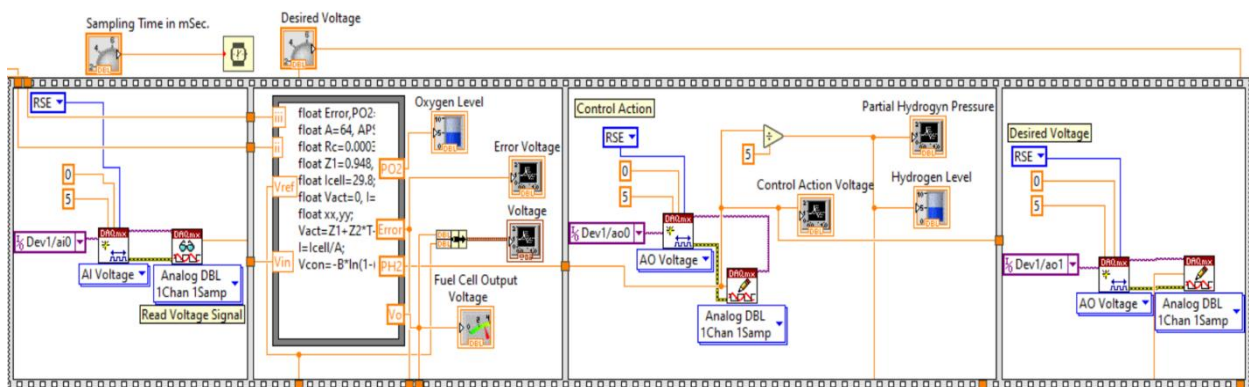


Figure. 5 Block diagram of the real-time PEMFC predictive controller in LabVIEW

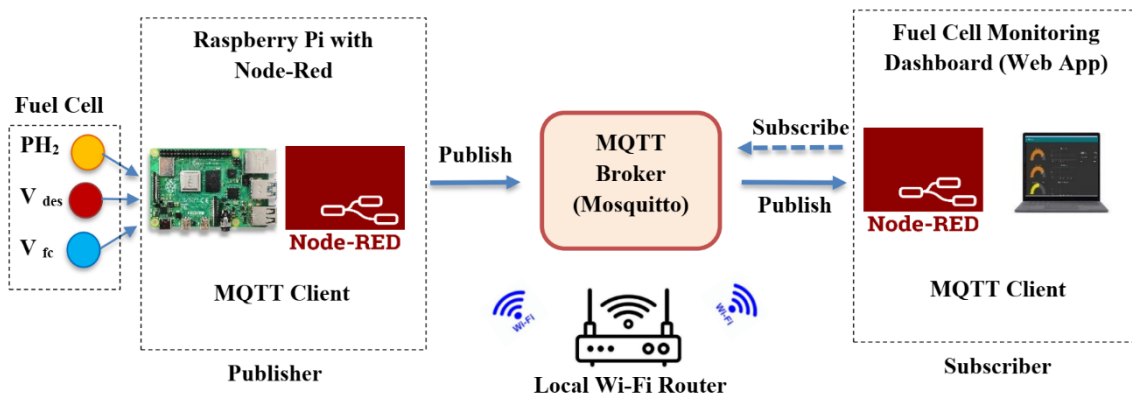


Figure. 6 MQTT protocol-based PEMFC monitoring system

illustrates the fundamental architecture of the MQTT. Typically, MQTT is a publish-subscribe protocol. It is a straightforward and compact messaging solution designed for unreliable networks, constrained hardware, and limited bandwidth. It is a suitable option for this architecture since it provides simple communication between the server (an MQTT broker) and clients (a Raspberry Pi-single board computer, computers, and mobile devices) [25].

After establishing a connection with an MQTT broker, a message related to a topic is published by an MQTT client. The broker sends the message to clients

who have subscribed to the relevant topic [26]. Consequentially, the primary purpose of the MQTT protocol in this work is to receive operational data from the fuel cell control system through the Raspberry Pi and transmit it to the MQTT client (a computer with a Node-RED monitoring dashboard).

Eclipse Mosquitto is used as a broker on the Raspberry Pi 4. Briefly, Mosquitto is an open-source message broker, which is a lightweight MQTT broker that can be used on all devices, including full servers and low-power boards, to publish and subscribe for messages [27]. The board being utilized is a

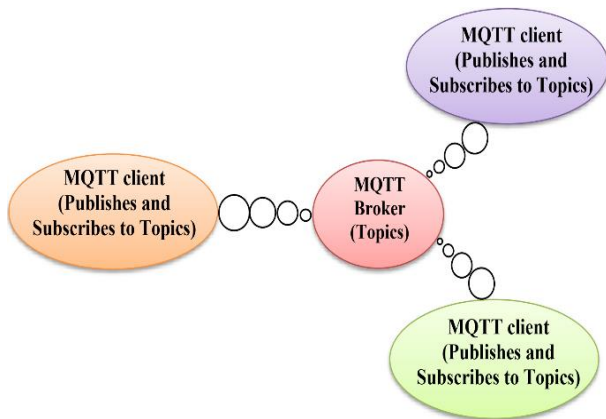


Figure. 7 The MQTT architecture

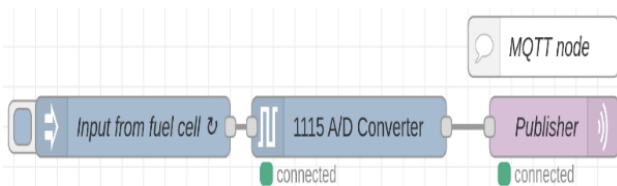


Figure. 8 Node-RED flow for PEMFC data publishing (in Raspberry Pi)

Raspberry Pi 4 Model B with a 1.5 GHz 64-bit quad-core ARM Cortex-A72 processor, full gigabit Ethernet, Bluetooth 5, two USB 2.0 ports, two USB 3.0 ports, 2 GB of RAM, and dual-monitor compatibility through a pair of mini-HDMI connections.

The Pi 4 is powered using a USB-C connection, which also powers connected peripherals in the downstream direction [28]. In a local network, the Raspberry Pi serves as the local server and hosts the MQTT broker (Mosquitto), and the Node-RED application. In this study, the required fuel cell data was collected using the Raspberry Pi 4. Essentially, for representing and visualizing fuel cell data, Node-

RED dashboards have been used. Node-RED is a flow-based programming tool that IBM originally created for the IoT to connect physical components, APIs, and web services. An online flow editor for Node-RED is available for writing JavaScript functions. Applications' components can be shared or saved for later use. Node.js is used to build the runtime and JSON is used to store the Node-RED flows [20].

Since the Raspberry Pi 4 has no analog inputs, we have used the ADS 1115 analog-to-digital converter to tap analog inputs from the fuel cell control system and convert them to a digital output. The ADS1115 is a 16-bit analog-to-digital converter with four analog input channels. We connect the ADS1115's SCL and SDA pins to the Raspberry Pi 4's digital GPIO (SCL and SDA) pins so that the Raspberry Pi 4 can receive the data needed for monitoring the fuel cell. Fig. 8 shows the Node-RED flow for PEMFC data publishing on the Raspberry Pi 4, which presents the ADS1115 node and the MQTT output node that is used to send data needed to monitor the FC to the Mosquitto broker.

On the other hand, Fig. 9 displays the Node-Red flow for PEMFC data subscription (on the laptop), which uses MQTT input nodes as subscribers to receive PEMFC monitoring data from the broker. In this regard, one of the most noticeable features of Node-Red is the dashboard module, which is a web-based data monitoring tool [29]. Three different user interface types (gauge, text, and chart) are displayed by the Node-RED dashboard in the presented work, including the FC output voltage, the FC desired voltage, and the hydrogen partial pressure control action that are each depicted on the fuel cell monitoring dashboard in these three different forms of the user interface.

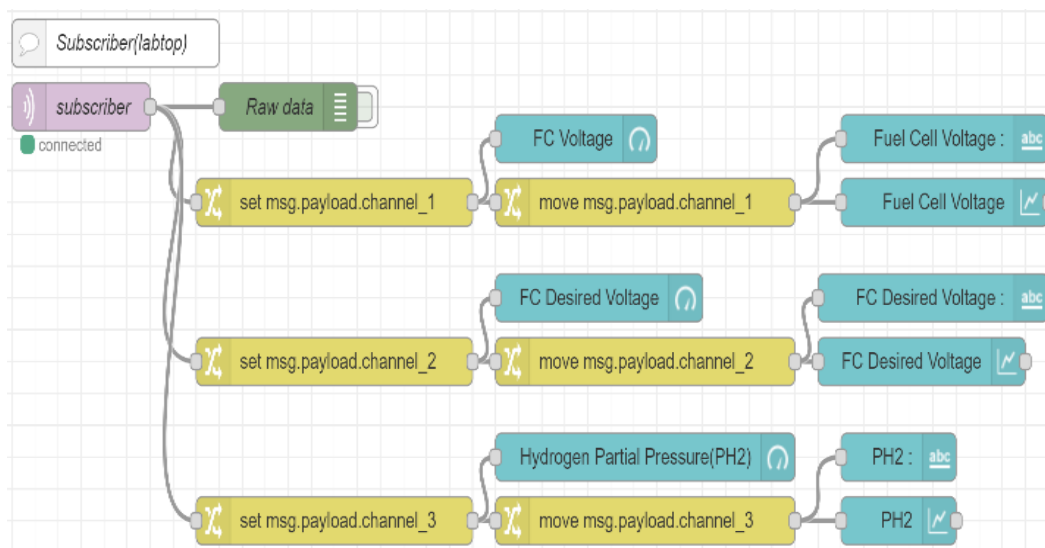


Figure. 9 Node-RED flow for PEMFC data subscription (Laptop)

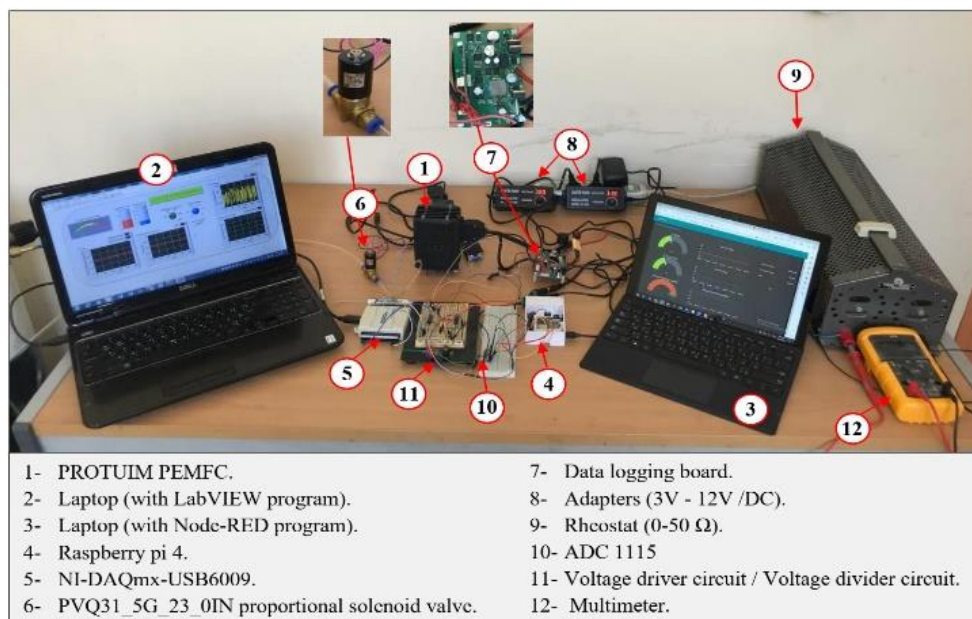


Figure. 10 Hardware setup for the experimental work

#### 4. Experimental setup

The primary hardware component of the proposed experimental work is the PROTIUM's PEM fuel cell device, where the mechanism of a chemical reaction inside each cell is the operating principle of a PEMFC model. It is utilized to carry out the experimental work to investigate the relationship between the intended output voltage from the PEM fuel cell and the hydrogen partial pressure. The fuel cell requires a dry hydrogen gas that is 99.99% pure as fuel, and it requires a supply voltage between (12 to 15) volts to begin operating. In order to deliver the oxygen partial pressure needed to complete the chemical reaction, two fans are linked within the fuel cell body. Fig. 10 depicts an illustration of the hardware architecture. To accomplish the objective of this experimental work, all of the hardware stage's components are linked firstly, as depicted in Fig. 10, and the schematic diagram is presented in Fig.2. Secondly, in accordance with PROTIUM's specifications, the pressure in the hydrogen gas tank is set to 1 bar using the pressure regulator, and it cannot be raised over 1 bar to prevent breaking of the membrane that resides between the two poles.

The proposed predictive controller implemented in LabVIEW is used to determine the appropriate amount of PH<sub>2</sub> control action based on the desired voltage in steady state using Eq. (9). Then, the power supply is turned on to start the work by powering both cards of the fuel cell and the PVQ31\_5G\_23\_0IN proportional solenoid valve to carry on with this work. After that, the hydrogen gas enters the fuel cell from a hydrogen controlling the amount of PH<sub>2</sub> control

action that should be injected into the fuel cell is the major responsibility of this valve.

The tank through a digitally modulated valve, which is controlled by an electric signal with a range of (0 to 12) volts. proposed predictive controller that runs on LabVIEW drives provides the PH<sub>2</sub> control action for the valve through the NI USB 6009. The NI USB-6009 is a lightweight, multifunctional data acquisition (DAQ) device made by national instruments, which is compatible with LabVIEW. It is utilized in the experimental work for the interface between a personal computer and a fuel cell. The H<sub>2</sub> gas and O<sub>2</sub> combine to produce electricity in a fuel cell stack. Then, the load receives the electricity produced. The load in this experimental study is a Rheostat, which is an electrical instrument that has a variable resistance and a resistivity range of up to 50 ohms. It has a volume to increase the load delivered to the PROTIUM PEM fuel cell, and it is used to regulate the current to adjust the voltage of the fuel cell. Then, the fuel cell output voltage signal goes to LabVIEW through the Rheostat to the voltage divider circuit. Then, the analog signal is converted to a digital signal using the ADC of the NI 6009 USB to monitor and control the output voltage. At the same time, the fuel cell output voltage goes to the Raspberry Pi 4. The ADS1115 is used to pass the analog FC output voltage signal along with the PH<sub>2</sub> control action and the FC desired voltage to the Raspberry Pi 4, as seen in Fig. 2. Here, the Node-RED application running on the Raspberry Pi 4 serves as an MQTT client (publisher), gathering the necessary data about the fuel cell and publishing it to the MQTT broker on a particular topic.

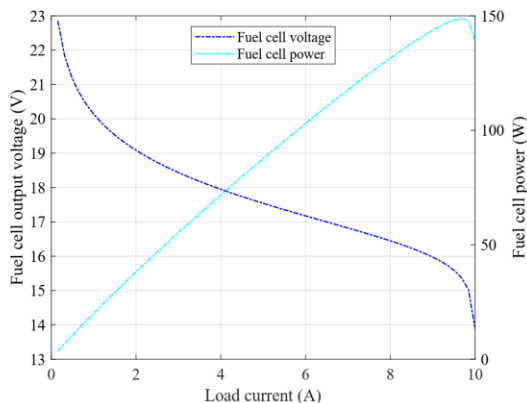


Figure. 11 The stack output voltage and power against the current

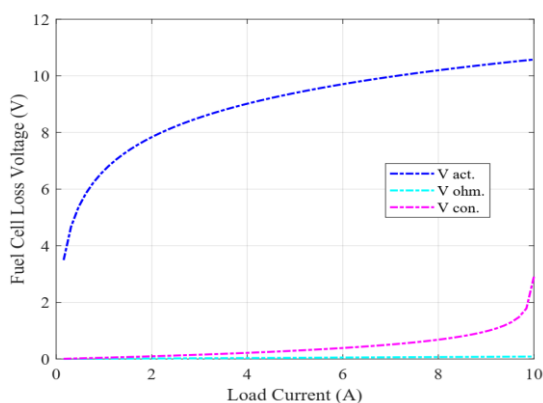


Figure. 12 Fuel cell voltage drop against the load current

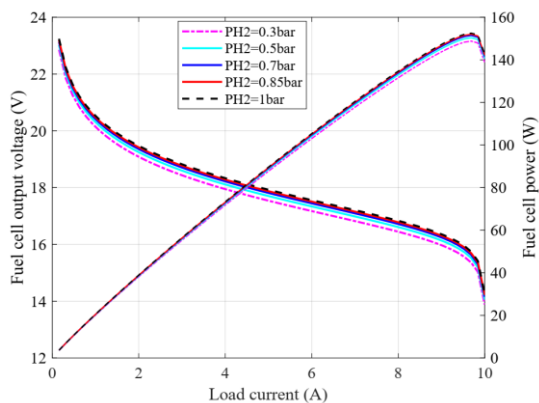


Figure. 13 The maximum power and the output voltage against the load current with variable hydrogen partial pressure

The Raspberry Pi 4 then functions as a local server with the MQTT broker (Mosquitto Server) running on it. The gathered data is sent wirelessly through Wi-Fi from a nearby router to the subscriber. On the other hand, a personal computer (laptop) running the Node-Red web application subscribes to that subject in order to obtain the necessary fuel cell information and display and monitor it in the form of charts, text, and gauges on the Node-RED dashboard.

### 5. Simulation and experimental results

The PEMFC nonlinear model was investigated and analysed, as was the proposed predictive controller, which was validated and built using the MATLAB R2020a package and Intel Core i5 computer hardware, which has a RAM capacity of eight gigabytes and a clock speed of 1.50 GHz. The PROTIUM Company's PEM fuel cell was used in this study to conduct the experimental work and examine the link between the intended output voltage from the PEM fuel cells and the hydrogen partial pressure. The study and analysis of the PEMFC system's dynamic properties were performed in relation to its physical parameters, as shown in Table 1, which is necessary to demonstrate the nonlinear dynamic behaviour of the fuel cell model, and these are the first steps in the proposed system design. The first analysis is: The magnitude of the fuel cell's output voltage and the maximum output power response are depicted in Fig. 11, where the fuel cell model's normal operating conditions are: (1) The value of the hydrogen partial pressure is equal to 0.3 bar; (2) The value of the oxygen partial pressure is equal to 0.2 bar; (3) The operating temperature of the fuel cell model is equal to 25 °C. Under load, the fuel cell's load current is variable between 0 and 10 A; this is the model's maximum power of 150 watts. The loss voltage response of the fuel cell system is shown in Fig. 12 when the variable load current, which is adjustable between 0 A and 10 A, is applied. In the second analysis, which is shown in Fig. 13, the fuel cell can be operated while the load current varies between 0 A and 10 A to show the effect of the hydrogen partial pressure varying between 0.3 bar and 1 bar on the output voltage as well as the maximum output power. However, at 25 °C, the fuel cell's operating temperature never changes. According to Fig. 13, the output voltage of the fuel cell rises as the hydrogen partial pressure does. The enhanced thermodynamic potential value of the PEMFC system, as given in Eq. (7), has improved the dynamic performance of the fuel cell system's output voltage.

According to Fig. 14, which depicts the effect of temperature variations on a fuel cell system, the temperature varies from 25 °C to 80 °C while the fuel cell's load current fluctuates between 0 A and 10 A, while the partial pressures of hydrogen and oxygen remain constant at 1.0 bar and 0.2 bar, respectively. As the temperature rises, the FC's output voltage improves. The performance of the fuel cell system has been improved by enhancing the  $E_N$  value of the PEMFC system to increase and lower the parameter impact values on the loss voltage. However, as the

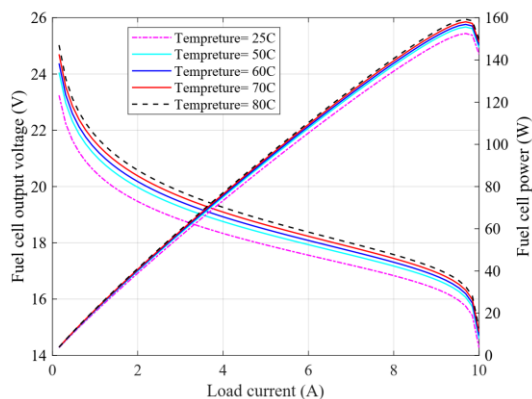


Figure. 14 The stack output voltage and power against the load current with temperature

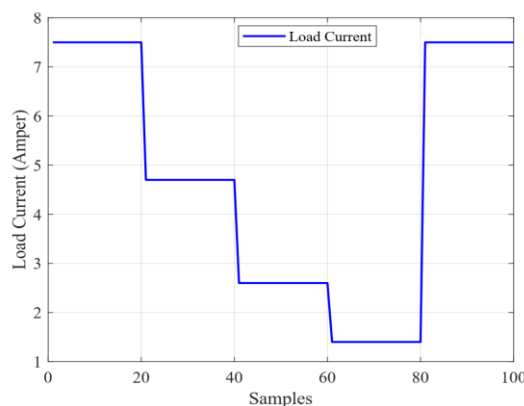


Figure. 17 The output load current for the PEMFC using the one-step-ahead predictive voltage controller

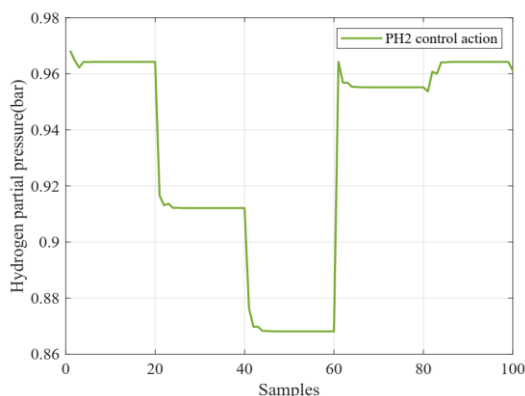


Figure. 15 The response for the one-step-ahead prediction control action PH<sub>2</sub>

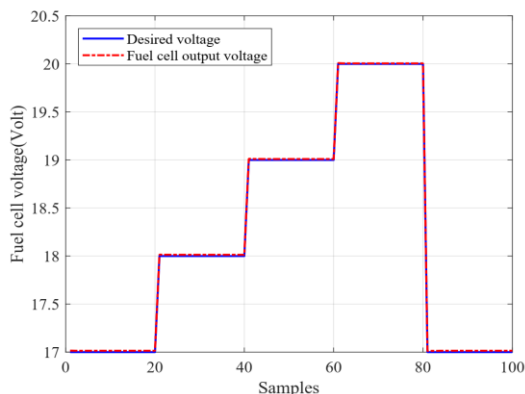


Figure. 16 PEMFC system's actual output voltage for the one-step-ahead predictive voltage controller

temperature rises, the fuel cell's lifetime will be shortened because it will operate with a fewer value of the necessary humidity for the membranes.

Predictive neural voltage control, as seen in Fig. 3, was used to improve the dynamical behaviour of the output voltage of the nonlinear PEMFC system. This can be accomplished by regulating the PEMFC output voltage in the presence of current variation and by forecasting the best PH<sub>2</sub> values to protect the fuel cell membrane from damage in such a way that

Table 2. The study cases for the experimental work

Case study	FC output voltage	Load current	Rheostat Resistance	FC Power
1	17 V	7.5 A	2.2 Ω	123.7 W
2	18 V	4.7 A	3.8 Ω	83.9 W
3	19 V	2.6 A	7.3 Ω	49.3 W
4	20 V	1.4 A	14.2 Ω	27.8 W

extends the fuel cell lifetime without consuming a lot of PH<sub>2</sub>.

Fig. 15 shows the one-step-ahead prediction response of the control action of the proposed predictive neural controller based on Eq. (9). The PEMFC system's target output voltage is followed quickly and smoothly in the optimal response of the PH<sub>2</sub> control action, roughly minimizing both steady-state and transient deviations from zero. The one-step-ahead predictive neural controller's real output voltage for the PEMFC system is shown in Fig. 16, which also shows that the response is quick and smooth so as to follow the fuel cell model's desired output voltage.

Fig. 17 displays the output load current response for the fuel cell according to the suggested predictive controller.

Four study cases were selected, as shown in Table 2, in order to test the effectiveness of the suggested predictive controller for the fuel cell system in real time. The LabVIEW 2020 package was then used to track and control the fuel cell output voltage and the control signal for 100 samples with a sampling interval of one second.

Figs. 18 (a), (b), (c), and (d) show the first case. After reducing the output voltage from 17 volts to a suitable voltage range of (3 to 5) volts based on the voltage divider circuit and with 7.5 amps of the load current response when the resistance is applied at a value of 2.2 Ω on the rheostat, Fig. 18 (a) shows the

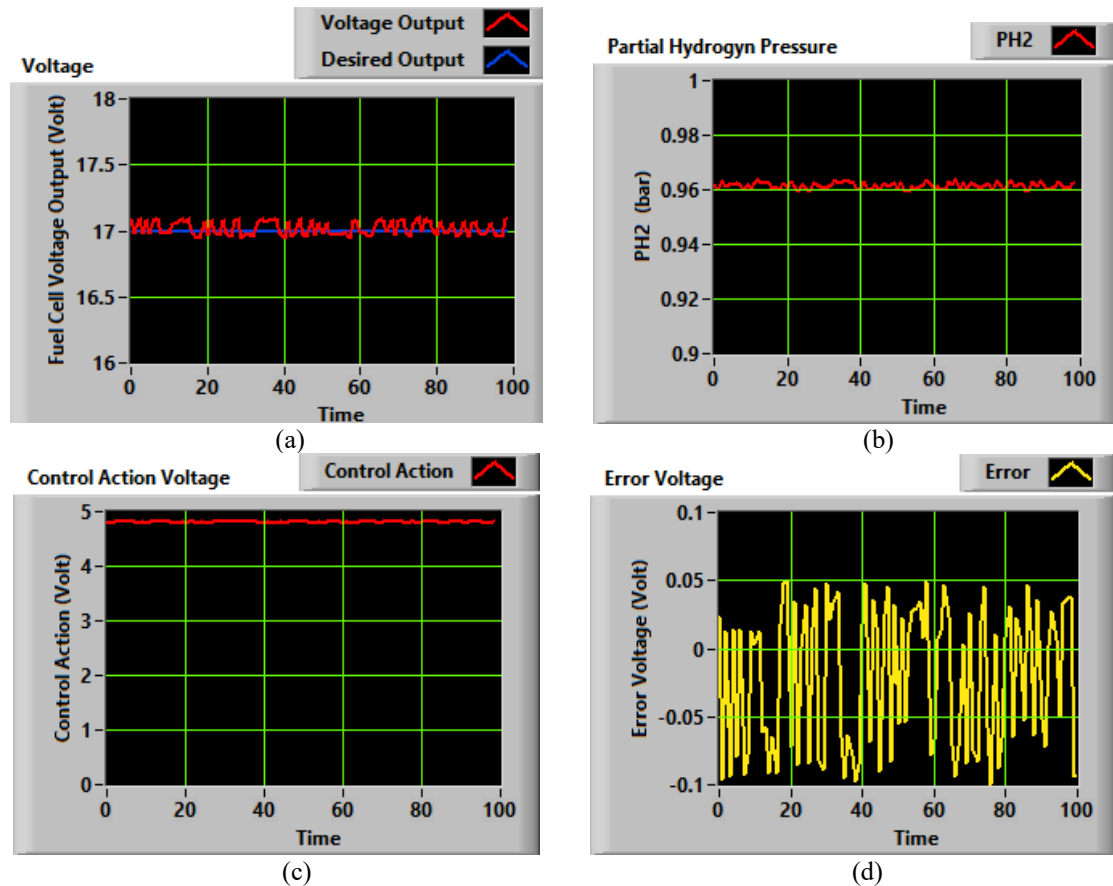


Figure. 18 Case study one for the desired voltage at 17 volts: (a) The actual output voltage response of the PEM fuel cell, (b) The hydrogen partial pressure control action, (c) The voltage-control action response, and (d) The PEM fuel cell voltage error for the proposed closed-loop controller

real response of the fuel cell output voltage with the intended voltage of 17 volts and using the first channel ADC for the NI-DAQmx-USB6009 device to read this voltage signal. In the steady state, the response of the output voltage is rapid and stable, exhibiting minimal oscillation of approximately  $\pm 0.1$  volts.

This oscillation is caused by a number of factors that have an impact on the measurement process, including the noise effect, the fuel cell's uncertain system parameter fluctuations, and the impurity of the hydrogen gas. The proposed predictive neural controller's PH<sub>2</sub> control action of a one-step-ahead prediction response is shown in Fig. 18 (b). The best value, quick, and smooth control action to follow the target output voltage of the PEMFC system is included in the optimal response of the PH<sub>2</sub> control action, with small oscillation, which roughly minimizes the steady-state deviation from zero.

The proportional solenoid valve voltage control action of the predictive neural controller is shown in Fig. 18 (c). It was sent from the first channel DAC of the NI-DAQmx-USB 6009 with a range of (0 to 5) volts using a diver circuit (operational amplifiers) to raise the value of the control signal to a range of (0 to

12) volts to operate the proportional solenoid valve of type PVQ31\_5G\_23\_0IN. The controller has a quick response time for reaching the desired voltage and stabilizing it with a minimum amount of oscillation in the steady state.

The voltage error in steady states is depicted in Fig. 18 (d), which is about 0.1 volts.

Figs. 19 (a), (b), (c), and (d) display the results of the second case study. Figure 19 (a) shows the real-time output voltage of the fuel cell when the resistance of the load is applied at a value of  $3.8 \Omega$  on the rheostat, with the desired voltage at 18 volts and to make 4.7 amps of the load current response. The output voltage responds quickly and steadily in the steady state, with just a small oscillation of about  $\pm 0.1$  volts.

Fig. 19 (b) displays the PH<sub>2</sub> control action of the proposed predictive neural controller, demonstrating a one-step-ahead prediction response. The controller exhibits an optimal response, ensuring a precise and smooth control action to track the target output voltage of the PEMFC system and minimizing steady-state deviation from zero. The proportional solenoid valve voltage control action of the predictive neural controller is depicted in Fig. 19 (c), which

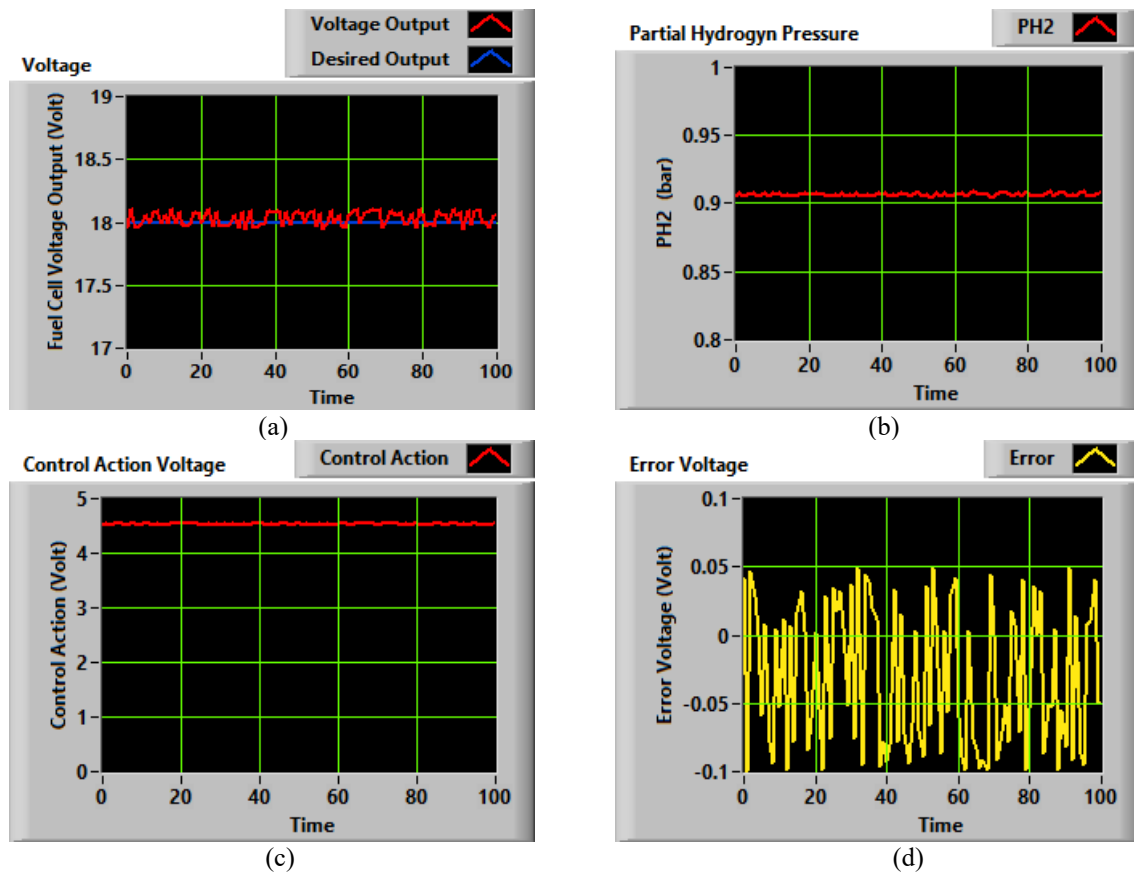


Figure. 19 Case study one for the desired voltage at 18 volts (a) The actual output voltage response of the PEM fuel cell (b) The hydrogen partial pressure control action (c) The voltage-control action response (d) The PEM fuel cell voltage error for the proposed closed-loop controller

shows a rapid time response to reach the desired voltage and stabilize it with minimal oscillation in the steady state. The voltage error in steady states is shown in Fig. 19 (d), which is around 0.1 volts.

Figs. 20 (a), (b), (c), and (d) depict the third case study. Fig. 20 (a) shows the real output voltage response of the fuel cell model with the intended voltage at 19 volts, and to make the load current equal to 2.6 amps, the resistance of the rheostat is applied at a value of  $7.3 \Omega$ . The output voltage response is fast, and in the steady state, there is a small output oscillation of about  $\pm 0.1$  volts. The proposed predictive neural controller's  $\text{PH}_2$  control action of the one-step-ahead prediction response is shown in Fig. 20 (b). The best value, quick, and smooth control action to follow the target output voltage of the PEMFC system is included in the optimal response of the  $\text{PH}_2$  control action with a small oscillation. The proportional solenoid valve voltage level control action of the predictive neural controller is shown in Fig. 20 (c). The controller has a quick response time for reaching the desired voltage and stabilizing it with a minimum amount of oscillation in the steady state of about  $\pm 0.1$  volts. The voltage error in steady states is depicted in Fig. 20 (d), which is about 0.1

volts.

Figs. 21 (a), (b), (c), and (d) depict the fourth case study. In particular, Fig. 21 (a) demonstrates the behavior response of the actual output voltage of the fuel cell in real-time with the intended voltage at 20 volts and 1.4 amps of the load current response when the resistance is applied at a value of  $14.2 \Omega$  on the rheostat. The output voltage response is quick, and in the steady state, there is a small output oscillation of about  $\pm 0.1$  volts. The proposed predictive neural controller's  $\text{PH}_2$  control action of the one-step-ahead prediction response is shown in Fig. 21 (b). The proportional solenoid valve voltage level control action of the predictive neural controller is shown in Fig. 21 (c). The voltage error in steady states is depicted in Fig. 21 (d), which is about 0.1 volts.

Upon conducting these four case studies, the efficacy of the proposed predictive neural controller has been validated. It has been established that the simulation results align with the experimental findings in terms of providing a rapid and accurate response as well as generating an optimal hydrogen partial pressure control action that regulates the fuel cell output voltage during current variations.

Nevertheless, there is a minor voltage error and a

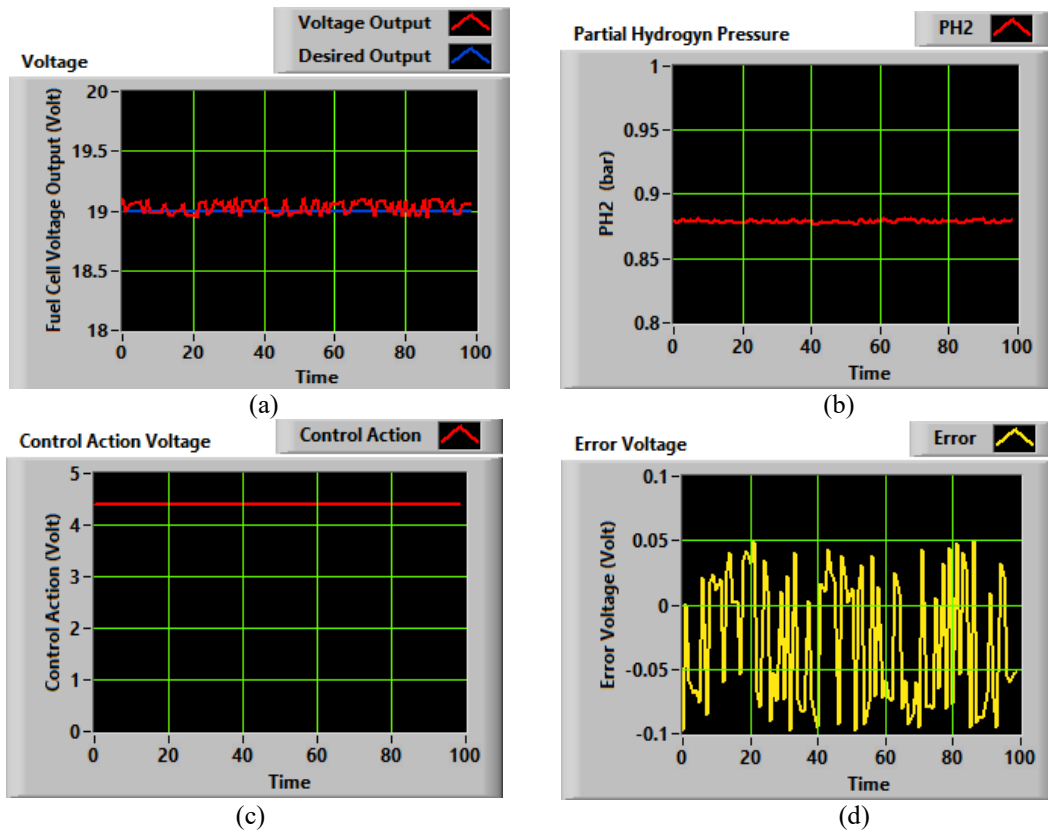


Figure. 20 Case study one for the desired voltage at 19 volts (a) The actual output voltage response of the PEM fuel cell (b) The hydrogen partial pressure control action (c) The voltage-control action response (d) The PEM fuel cell voltage error for the proposed closed-loop controller

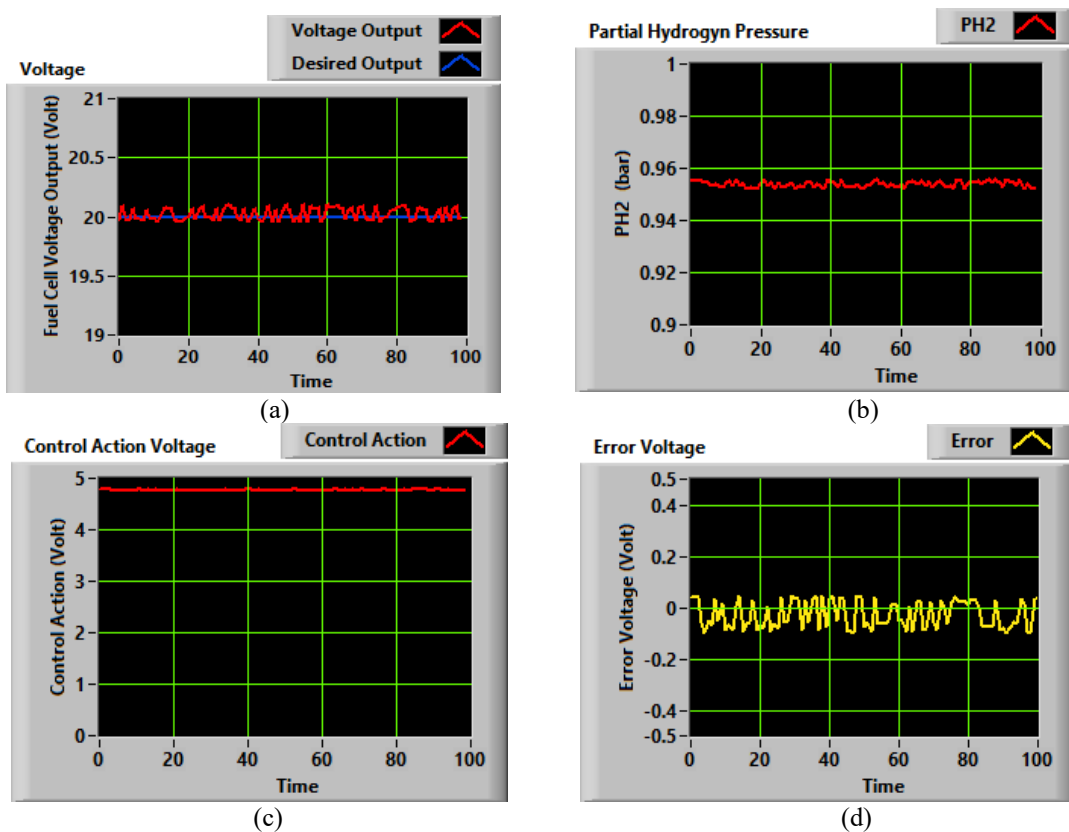


Figure. 21 Case study one for the desired voltage at 20 volts: (a) The actual output voltage response of the PEM fuel cell, (b) The hydrogen partial pressure control action, (c) The voltage-control action response, and (d) The PEM fuel cell voltage error for the proposed closed-loop controller

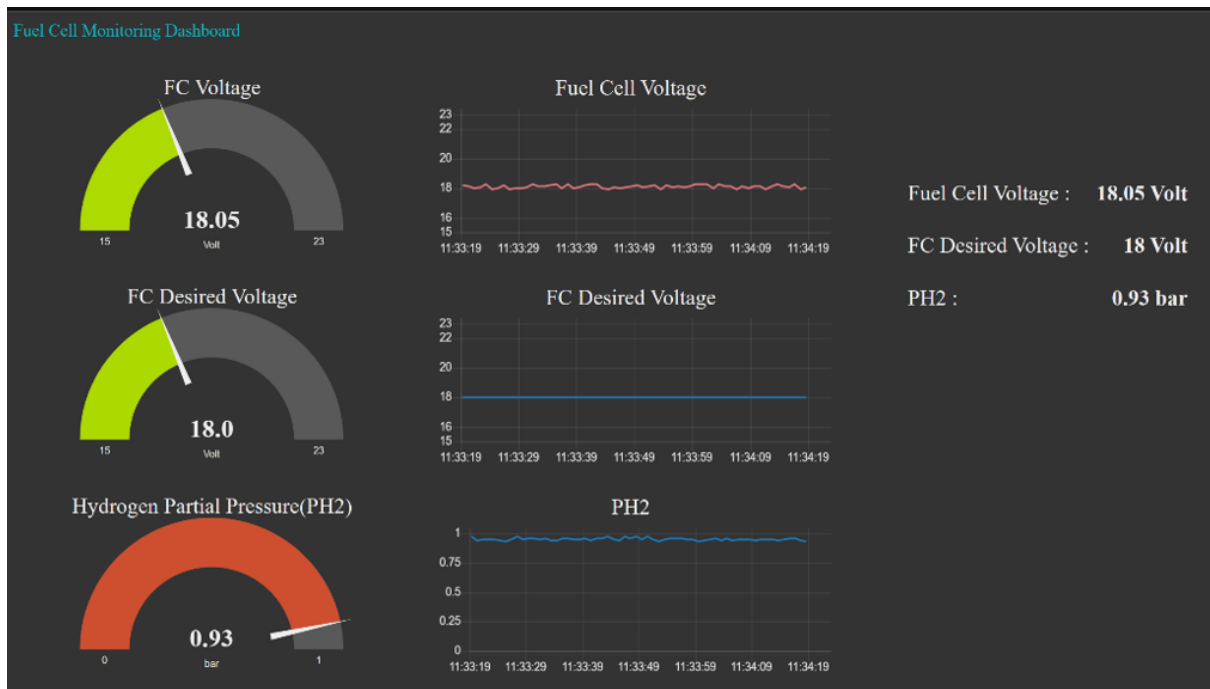


Figure. 22 The node-red dashboard for real-time PEMFC monitoring

Table 3. Validation of the experimental results

Result type	Voltage error	Oscillation
Numerical simulation	0.01	No oscillation
Experimental work	0.1	$\pm 0.1$

slight oscillation, which can be attributed to various factors affecting the measurement process. These factors include the influence of noise, fluctuations in uncertain system parameters of the fuel cell, and impurities in the hydrogen gas. The Node-RED dashboard for real-time PEMFC monitoring is displayed in Fig. 22, which displays gauges, text, and charts showing the actual fuel cell output voltage, the intended voltage, and the hydrogen partial pressure using Ch0, Ch1, and Ch2 of the ADC-1115, respectively for the case study with a desired voltage of 18 volts, where the value of the desired output voltage is taken from the second channel DAC of the NI 6009, while the value of the control voltage signal is taken from the first channel DAC of the NI 6009.

In a local area network (LAN) network, this information is sent from the Raspberry Pi to a remote laptop based on the MQTT communication protocol and the local wi-fi router. By using a single panel, this dashboard allows us to track the operation of the PEMFC control system in real time.

In Table 3, to validate the effectiveness of the proposed experimental work, the simulation results were compared with those of the experimental work.

The differences between the simulation findings and the experimental results can be attributed to few

Table 4. Comparing the suggested controller numerically to other types of controllers

Type of Controller	Algorithm	Voltage Error	Oscillation
Predictive neural controller 1-10 step ahead [16]	CPSO (Off-line)	0.08	$\pm 0.05$
NARMA-L2 inverse neural controller [13]	FF	0.09	$\pm 0.17$
	CPSO	0.083	$\pm 0.12$
	FFCPSO (On-line)	0.055	$\pm 0.1$
The proposed predictive control law equation	BPA (On-line)	0.01	No oscillation

points that were not addressed in the simulation results, including the following:

- The PH<sub>2</sub> solenoid valve model was neglected.
- The quantization error resulting from arithmetic operations of the ADC and DAC.
- The hydrogen gas impurity. Since the PROTIUM PEMFC employed in the experimental study requires a dry hydrogen gas that is 99.99% pure as fuel.
- The driver circuits of the operational amplifiers have some offset voltage value or a drift voltage in the output.
- The errors in fuel cell modeling and the absence

of full comprehension of system components.

We were able to compare the numerical simulation results of the proposed controller with those of other types of controllers based on improving system performance in terms of swiftly and precisely tracking the desired voltage and using less energy by analysing and contrasting the PEMFC system under random current fluctuations and a low voltage tracking error as shown in Table 4.

The proposed controller was initially compared to the research in [16], which recommended using a neural predictive controller with CPSO to determine the action of the hydrogen partial pressure to maintain the target output voltage of the PEMFC system during variations in the load current. The actual output voltage of the PEMFC system for the input set used by our suggested controller and obtained from [16] is shown in Fig. 23. One step ahead, the ideal answer will be reached. The enhancement of the voltage tracking error was 87.5%, and the tracking voltage error was reduced from 0.08 to 0.01 volt. Even though the actual output voltage of the PEMFC system in [16] could follow the desired output for one-step-ahead prediction for five different load current step-changes with small output oscillation, the voltage error was not equal to zero at steady state, it caused overshoot response in the start sample, and it did not result in a smooth response to the control action (hydrogen partial pressure).

Because it created the ideal or nearly optimal control action based on the predictive control law equation with the neural network identification as a guide, the suggested predictive neural controller produced superior control performance. The suggested predictive controller, however, relies on the MERNN identifier network, which has [8:8:8:1] nodes, including eight nodes for input, context, and hidden layers, an output layer, and one node for the output layer. The PH<sub>2</sub> control action in [20] was produced using just the feedback neural controller that used the traditional MLP identification model, which has [5:7:1] nodes.

The results from [13], which introduced the neural network NARMA-L2 structure model and the hybrid (FF-CPSO) firefly-chaotic particle swarm optimization algorithm that was used to build the model and control system for the nonlinear PEMFC model, were compared with those of the suggested predictive methodology as part of a second comparative study. The best response will be attained, where the voltage error is decreased from 0.055 volts to 0.01 volts and the tracking voltage error is boosted by 81.8%, if the identical input that has been obtained from [13] is applied to our suggested controller.

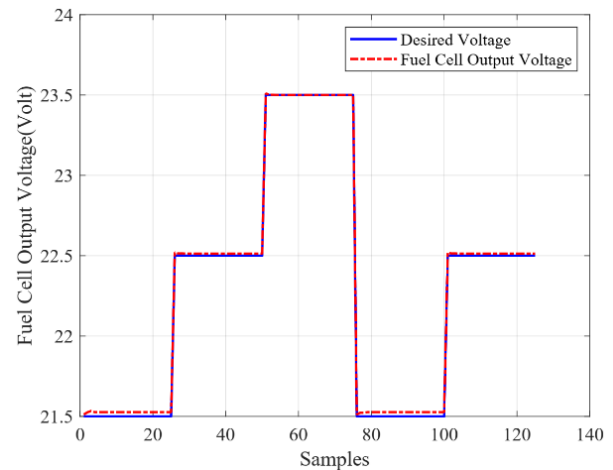


Figure. 23 FC output voltage based on the data set [16]

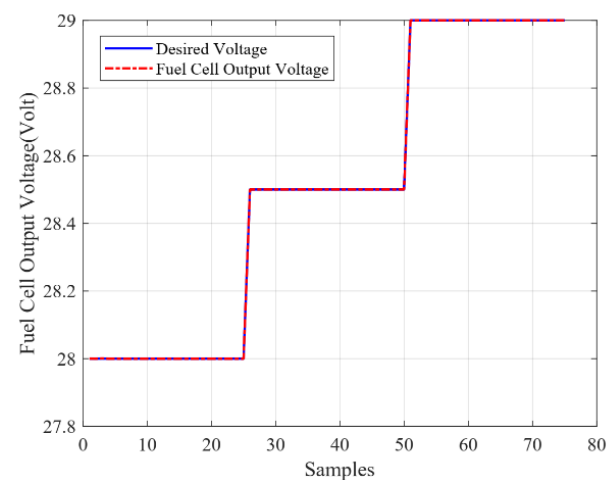


Figure. 24 FC output voltage based on data set [13]

There is no longer any oscillation effect at all. The PEMFC system's actual output voltage for the input set chosen from [13] is shown in Fig. 24.

The suggested predictive neural controller creates the control action based on both the feedback neural controller and the predictive control law equation, which is how this superiority was reached. In [13], the controller only relied on the inverse neural controller to provide the control action. This controller provides accurate responses in the steady state but produces mistakes in the transient state.

## 6. Conclusion

In this study, a real-time predictive voltage neural controller and remote monitoring are constructed for the nonlinear PEMFC system. In order to optimize the fuel cell's nonlinear performance under different load currents and to enable remote monitoring of the nonlinear PEMFC system, the main goal of this work is to precisely and quickly establish the best control action for the hydrogen partial pressure. The

proposed predictive voltage controller is applied to the 150-watt PROTIUM PEMFC in order to check the performance of the device in real time using the LabVIEW package.

As shown by the MATLAB simulation results and the experimental work in real time based on the LabVIEW program and the Node-RED web application, the performance of the suggested monitoring and control system clearly demonstrates the following capabilities:

- According to the simulation results using the MATLAB toolkit, applying the suggested one-step-ahead predictive neural controller to the 150-watt PROTIUM PEMFC results in smooth, quick, and precise control action without oscillation with fast tracking of the desired output voltage with roughly 0.01 voltage error during load current variation.
- The proposed predictive controller's real-time experimental implementation, which is based on the LabVIEW toolkit, demonstrates that it can generate the best  $\text{PH}_2$  control action with little oscillation and can track the desired voltage with a minimum error of about 0.1 volts with  $\pm 0.1$  volts oscillation.
- The difference between the simulation results and the experimental results is a consequence of certain factors that were not included in the simulation results, such as the fuel valve model being ignored, the impurity of the hydrogen gas, and the quantization error of the ADC and DAC.
- The established remote monitoring system, based on the Node-RED web application and the MQTT communication protocol, has been successfully implemented. It enables quick and accurate wireless LAN monitoring of the PEMFC control system's performance.

In future works, we advise using a real-time flying drone model with real-time power management as the experimental setting for the predictive control using IoT approach in further studies.

### Conflicts of interest

Considering the authors, there are no any conflicts.

### Author contributions

Ahmed Sabah Al-Araji explained the mathematical model of the fuel cell. Fatima Abdul Sattar Al-Taie and Ahmed Sabah Al-Araji

implemented the proposed predictive control law on LabVIEW. Fatima Abdul Sattar Al-Taie developed the remote monitoring system. Fatima Abdul Sattar Al-Taie and Ahmed Sabah Al-Araji applied the experimental setup and demonstrated the simulation results of this research.

### References

- [1] T. Wilberforce, H. Rezk, A. G. Olabi, E. I. Epelle, and M. A. Abdelkareem, "Comparative Analysis on Parametric Estimation of a PEM Fuel Cell using Metaheuristics Algorithms", *Energy*, Vol. 262, pp. 1-16, 2023.
- [2] F. A. S. A. L. Taie and A. S. A. Araji, "Development of Predictive Voltage Controller Design for PEM Fuel Cell System based on Identifier Model", *International Journal of Intelligent Engineering and Systems*, Vol. 16, No. 2, pp. 343-360, 2023, doi: 10.22266/ijies2023.0430.28.
- [3] M. A. Kamoona, O. C. Kivanc, and O. A. Ahmed, "Intelligent Energy Management System Evaluation of Hybrid Electric Vehicle based on Recurrent Wavelet Neural Network and PSO Algorithm", *International Journal of Intelligent Engineering and Systems*, Vol. 16, No. 1, pp. 388-401, 2023, doi: 10.22266/ijies2023.0228.34.
- [4] A. Djerioui, D. Ouali, and M. Ladjal, "Sliding Mode Control Using SVM for Power Quality Enhancement in Stand-Alone System based on Four-Leg Voltage", *International Journal of Intelligent Engineering and Systems*, Vol. 11, No. 2, pp. 266-274, 2018.
- [5] W. T. J. A. Rubaye, A. S. A. Araji and H. A. Dhahad, "Design and Implementation of Digital Controller for Fuel Cell System based on FPGA Technique", *Journal of Xi'an University of Architecture & Technology*, Vol. 12, No. 6, pp. 1106-1122, 2020.
- [6] A. Goshtasbi, B. L. Pence, J. Chen, M. A. D. Bolt, C. Wang, J. R. Waldecker, S. Hirano, and T. Ersal, "A Mathematical Model Toward Real-Time Monitoring of Automotive PEM Fuel Cells", *Journal of The Electrochemical Society*, Vol. 167, No. 2, pp. 1-22, 2020.
- [7] E. López, J. Monteiro, P. Carrasco, J. Sáenz, N. Pinto, and G. Blázquez, "Development, Implementation and Evaluation of a Wireless Sensor Network and a Web-Based Platform for the Monitoring and Management of a Microgrid with Renewable Energy Sources", In: *Proc. of International Conference on Smart Energy Systems and Technologies (SEST), IEEE*, pp. 1-

- 6, 2019.
- [8] H. Chang and P. Thapa, "A Study of Monitoring and Operation for PEM Water Electrolysis and PEM Fuel Cell Through the Convergence of IoT in Smart Energy Campus Microgrid", *Journal of the Korea Convergence Society*, Vol. 7. No. 6, pp. 13-21, 2016.
- [9] S. Qi, Y. Hu, X. Xue, and C. Sun "Remaining Useful Life Estimation for PEMFC based on Monitoring Data", In: *Proc. of 32nd Youth Academic Annual Conference of Chinese Association of Automation (YAC)*, IEEE, pp. 608-612, 2017.
- [10] C. Ziogou, D. Giaouris, S. Papadopoulou, and S. Voutetakis, "Supervisory Control and Monitoring of a Hybrid High Temperature PEM Fuel Cell System with Li-Ion Batteries and an LPG Reformer", *Chemical Engineering Transactions*, Vol. 52, pp. 1021-1026, 2016.
- [11] K. Darowicki, E. Janicka, M. Mielniczek, A. Zielinski, L. Gawel, J. Mitzel, and J. Hunger, "Implementation of DEIS for Reliable Fault Monitoring and Detection in PEMFC Single Cells and Stacks", *Electrochimica Acta*, Vol. 292, pp. 383-389, 2018.
- [12] X. Lu, X. Miao, Y. Xue, L. Deng, M. Wang, D. Gu, and X. Li, "Dynamic Modeling and Fractional Order PI $\lambda$ D $\mu$  Control of PEM Fuel Cell", *International Journal of Electrochemical Science*, Vol. 12, pp. 7518 – 7563, 2017.
- [13] K. E. Dagher, "Design of an Adaptive Neural Voltage-Tracking Controller for Nonlinear Proton Exchange Membrane Fuel Cell System based on Optimization Algorithms", *Journal of Engineering and Applied Sciences*, Vol. 13, No. 15, pp. 6188-6198, 2018.
- [14] J. A. Flach and F. A. Farret, "Circuit for Monitoring and Reestablishment of PEM Fuel Cell Voltage Using Controlled Short Circuits", In: *Proc. of 2019 IEEE PES Innovative Smart Grid Technologies Conference, Latin America (ISGT Latin America)*, Gramado, Brazil, pp. 1-5, 2019.
- [15] C. Shou, C. Yan, J. Chen, L. Hong, R. Wu, and Z. Luo, "Condition Monitoring and Fault Diagnosis of PEMFC Systems", In: *Proc. of 2019 Chinese Automation Congress (CAC)*, Hangzhou, China, pp. 4787-4791, 2019.
- [16] A. S. A. Araji, H. A. Dhahad, and E. A. Jaber, "A Neural Networks based Predictive Voltage-Tracking Controller Design for Proton Exchange Membrane Fuel Cell Model", *Journal of Engineering*, Vol. 25, No.12, pp. 26-48, 2019.
- [17] C. Yan, J. Chen, H. Liu, L. Kumar, and H. Lu, "Health Management for PEM Fuel Cells Based on an Active Fault Tolerant Control Strategy", In: *Proc. of IEEE Transactions Conf. on Sustainable Energy*, Vol. 12, No. 2, pp. 1311-1320, 2021.
- [18] Y. Sun, L. Mao, K. He, Z. Liu, and S. Lu, "Imaging PEMFC Performance Heterogeneity by Sensing External Magnetic Field", *Cell Reports Physical Science*, Vol. 3, No. 10, 2022.
- [19] A. H. Mohammed, A. K. Shabeeb, and M. H. Ahmed, "Image Cryptosystem for IoT Devices Using 2-D Zaslavsky Chaotic Map", *International Journal of Intelligent Engineering and Systems*, Vol. 15, No. 2, pp. 543-553, 2022, doi: 10.22266/ijies2022.0430.48.
- [20] S. Chanthakit and C. Rattanapoka, "MQTT Based Air Quality Monitoring System using Node MCU and Node-RED", In: *Proc of 2018 Seventh ICT International Student Project Conference (ICT-ISPC)*, Nakhonpathom, Thailand, pp. 1-5, 2018.
- [21] H. A. Dhahad, K. E. Dagher, and A. S. A. Araji, "Design of Optimum SIMO-PID Neural Voltage Tracking Controller for non-Linear Fuel Cell System based on Comparative Study of Various Intelligent Swarm Optimization Algorithms", In: *Proc. of International Conf. on Sustainable Engineering and Technology (INTCSET 2020)*, Baghdad, Iraq, pp. 1-16, 2020.
- [22] A. S. A. Araji, M. F. Abbod, and H. S. A. Raweshidy, "Design of a neural predictive controller for nonholonomic mobile robot based on posture identifier", In: *Proc. of the IASTED International Conference on Intelligent Systems and Control*, Cambridge, United Kingdom, pp. 198–207, 2011.
- [23] I. G. Pérez, A. J. C. Godoy, J. M. P. Calero, and M. C. Godoy, "Monitoring Interfaces for Photovoltaic Systems and DC Microgrids: Brief Survey and Application Case", *XLII Jornadas de Automática*, pp. 183-189, 2021.
- [24] Y. A. Setiawan and A. Amirullah, "Implementation of Single-Phase DVR-BES Based on Unit Vector Template Generation (UVTG) to Mitigate Voltage Sag Using Arduino Uno and Monitored in Real-Time Through LabVIEW Simulation", *International Journal of Intelligent Engineering and Systems*, Vol. 14, No. 3, pp. 82-96, 2021, doi: 10.22266/ijies2021.0630.08.
- [25] A. Zare and M. T. Iqbal, "Low-Cost ESP32, Raspberry Pi, Node-Red, and MQTT Protocol Based SCADA System", In: *Proc. of 2020 IEEE International IOT, Electronics and Mechatronics Conference (IEMTRONICS)*, Vancouver, BC, Canada, pp. 1-5, 2020.

- [26] P. Gupta, K. V. V. Satyanarayan, and D. D. Shah, "Development and Testing of Message Scheduling Middleware Algorithm with SOA for Message Traffic Control in IoT Environment", *International Journal of Intelligent Engineering and Systems*, Vol. 11, No. 5, pp. 301-313, 2018, doi: 10.22266/ijies2018.1031.28.
- [27] R. K. Kodali and A. Anjum, "IoT based Home Automation using Node-RED", In: *Proc. of 2018 Second International Conference On. Green Computing and Internet of Things (ICGCIoT)*, Bangalore, India, pp. 386-390, 2018.
- [28] H. Ramzey, M. Badawy, M. Elhosseini, and A. A. Elbaset, "I<sup>2</sup>OT-EC: A Framework for Smart Real-Time Monitoring and Controlling Crude Oil Production Exploiting IIOT and Edge Computing", *Energies*, Vol. 16, No. 4, pp. 1-31, 2023.
- [29] S. A. Omid, M. J. A. Baig, and M. T. Iqbal, "Design and Implementation of Node-Red based Open-Source SCADA Architecture for a Hybrid Power System", *Energies*, Vol. 16, No. 5, pp.1-21, 2023.